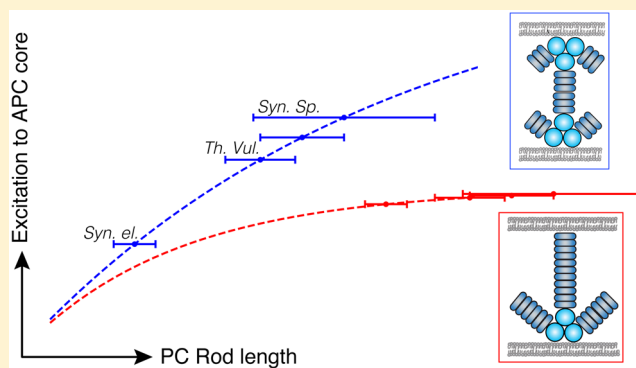


Light Adaptation in Phycobilisome Antennas: Influence on the Rod Length and Structural Arrangement

Aurélia Chenu,^{*,†,‡} Nir Keren,[§] Yossi Paltiel,[§] Reinat Nevo,^{||} Ziv Reich,^{||} and Jianshu Cao^{*,†,‡}[†]Massachusetts Institute of Technology, 77 Massachusetts Avenue, Cambridge, Massachusetts 02139, United States[‡]Singapore-MIT Alliance for Research and Technology, 138602 Singapore[§]Department of Plant and Environmental Sciences, Alexander Silberman Institute of Life Sciences, Givat Ram, The Hebrew University of Jerusalem, 91904 Jerusalem, Israel^{||}Department of Biomolecular Sciences, Weizmann Institute of Science, 7610001 Rehovot, Israel

Supporting Information

ABSTRACT: Phycobilisomes, the light-harvesting antennas of cyanobacteria, can adapt to a wide range of environments thanks to a composition and function response to stress conditions. We study how structural changes influence excitation transfer in these supercomplexes. Specifically, we show the influence of the rod length on the photon absorption and subsequent excitation transport to the core. Despite the fact that the efficiency of individual disks on the rod decreases with increasing rod length, we find an optimal length for which the average rod efficiency is maximal. Combining this study with experimental structural measurements, we propose models for the arrangement of the phycobiliproteins inside the thylakoid membranes, evaluate the importance of rod length, and predict the corresponding transport properties for different cyanobacterial species. This analysis, which links the functional and structural properties of full phycobilisome complexes, thus provides further rationales to help resolve their exact structure.



Photosynthetic organisms have evolved efficient strategies to harvest sunlight, directing the excitation through various molecular aggregates to the reaction center, where the light energy is converted into electrical and chemical energy. Among the primary producers, cyanobacteria, which can be viewed as the most important group of organisms ever to appear on our planet,¹ show great versatility in maintaining their structures. The cyanobacterial light-harvesting antenna, phycobilisome, is adapted to the particular environmental conditions, with drastic composition and function changes under stress conditions.^{2–4} Its high performance under drastically different living conditions has spurred investigations on the excitation transfer properties of this supercomplex.

The performance of light-harvesting antennas to transfer the electronic excitation to the reaction center is related to the spatial arrangement of the chromophores and proteins forming them, and many works have studied the transport properties in natural networks for a variety of organisms.^{5–12} Considering that increasing the area occupied by the chromophores increases the cross section to capture photons but decreases the transfer efficiency to the reaction center, an optimal efficiency is expected to be established for a particular ratio between donors (chromophores of the antenna) and acceptors (chromophores of the reaction center). Such observations have inspired the design of artificial networks¹³ and light-harvesting

devices,^{14–16} with promising applications in the development of organic solar cells^{17–19} and nano electronics.^{20,21}

Phycobilisomes (PBS) are mostly composed by the assembly of phycocyanin (PC), and sometimes phycoerythrin (PE), hexamers into rods, linked to a core formed by allophycocyanin (APC) trimers.²² The environmental factor that most influences the structure of PBS is light intensity, which can change the PC:APC ratio, and yield a maximum production of PC under optimal photon flux.²³ Other environment factors, such as light color and temperature, also influence the composition of the rods, changing the PC:PE ratio, either as an adaptation to the incident spectra^{24–26} or as a response to perturbed metabolic processes that regulates the synthesis of phycobiliproteins.

Here, we study the adaptation of the PC:APC ratio as a response to the light intensity, and combined with experimental measurements, we propose structural models for the arrangement of the PBS complexes in between the thylakoid membranes. To do so, we study the influence of the number of hexamers forming a homogeneous PC rod on the efficiency of excitation transport to the APC core. We first briefly describe

Received: August 4, 2017

Published: September 5, 2017

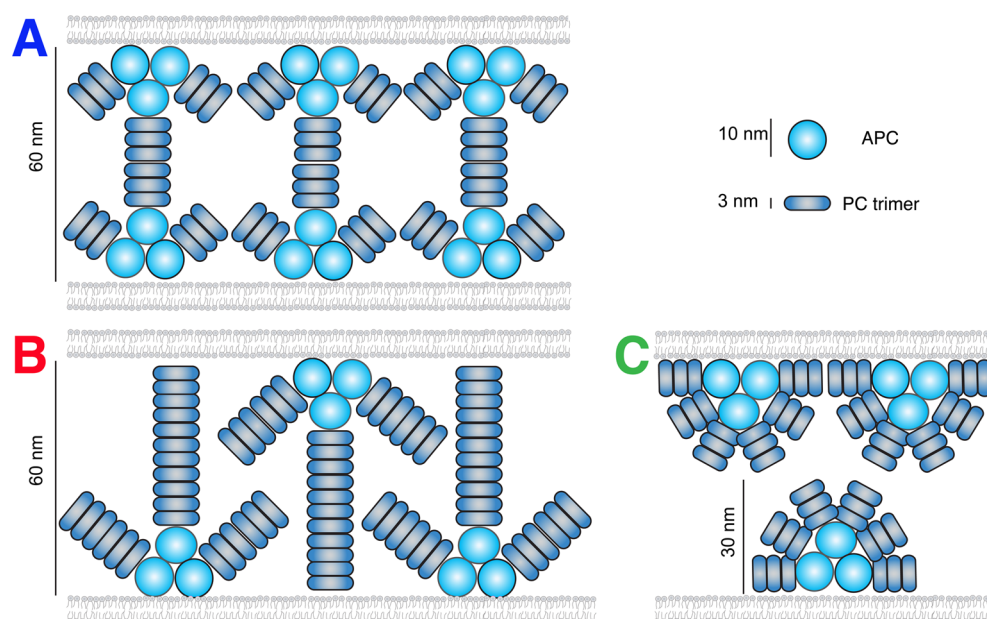


Figure 1. Cartoon of the proposed two limiting stacking models (A and B) of PBS units in the space between thylakoid membranes, along with the currently used model (C, adapted from ref 55). The length of the PC rod can be inferred from TEM images, and is given in Table 1 for different species.

the structure of phycobilisomes and their assembly properties. We then present the model and results of transport in the full aggregation state. In particular, we show how the amount of excitation transferred to the APC core can be kept constant under decreasing light intensity, increasing the PC rod length. We further provide different models for the structural arrangement of the PBS complexes, and compare the corresponding transport properties based on measurement for different cyanobacterial species.

■ STRUCTURE OF PHYCOBILIPROTEINS

The phycobilisomes^{22,27} consist of various types of bilin cofactors and pigment proteins, known as phycobiliproteins (PBPs), classified into four major groups: allophycocyanin (APC, $\lambda_{\max} = 652$ nm), phycocyanin (PC, $\lambda_{\max} = 620$ nm), phycoerythrin (PE, $\lambda_{\max} = 560$ nm), and phycoerythrocyanin (PEC, $\lambda_{\max} = 575$ nm). With the phycobilin chromophores being linear tetrapyrroles, they are conformally highly flexible, with optical and photophysical properties highly dependent on their environment. Hence, the pigment–protein interaction plays a crucial role in the function of PBP as an antenna complex, such that the chromophores' absorption and emission spectra in isolated state or denaturated PBP differ from the properties in intact form.

All PBPs are formed from a heterodimer primary building block, known as the ($\alpha\beta$) monomer, composed of two homologous subunits (α and β helices) and bilin cofactors, namely, α_{84} and β_{155} for APC, with an additional β_{84} chromophore for PC. The high degree of homology between the subunits and the monomer allows for further self-assemblies,²⁸ which leads to the formation of complex structures with controllable and efficient properties. PC, PEC, and PE associate into ($\alpha\beta$)₆ hexamers, and further stack into rods. APC trimers associate differently, forming cylinders from four trimers. These cylinders further pack into the core of the PBS. An APC core and rods made of stacked disks of PC and PE proteins further form a phycobilisome (Figure 1), which is

attached to the stromal side of the thylakoid membrane through the APC proteins in its core.

Compared to the Chl- and BChl-based antennas, the PBBS are characterized by large interchromophore distances. For example, in the minimal monomeric subunit of *Thermosynechococcus vulcanus*, the distance between the photosensitive bilins is 40 Å (between α – β) or 50 Å (β – β) (see Figure S1 in the Supporting Information). While assembly into trimer or hexamer results in more packed structures,²⁹ the distances (~20 Å) remain much larger than those in the chlorophyll-based antenna (e.g., those of green sulfur bacteria or plants have a typical distance of 10 Å). Despite the large distances, the transfer rates remain extremely efficient, with an overall quantum yield above 95%, which suggests that efficient transport does not require a high density of chromophores. While the energy transfer in PBS has been extensively studied on isolated subunits (e.g., see refs 30–33 and the rates in Table S1, Supporting Information), it is still unclear how further aggregation affects the energy flow. Very little is known of the excitation energy transfer at the level of rod aggregation, which we address here, in the framework of incoherent transfer.

■ EXCITATION TRANSFER IN PHYCOBILISOME RODS

We calculate the transfer of excitation along a linear rod of PC terminated by an APC trap, and study the transfer efficiency as a function of the homogeneous rod length and light intensity. We show that, for a given light intensity, there exists a rod length optimizing transfer to the core, and that the total excitation transferred to APC can be kept constant for different light intensities, by adjusting the rod length. The assumptions of our kinetic model are as follows: (i) we use incoherent, Förster theory considering that the distances between chromophores are large; (ii) we exclude back-transfer from the core to the rod due to the small spectral overlap of the components and the quick depopulation of APC;^{34,35} (iii) the spectral properties of each chromophore composing the PC trimers are assumed to be identical throughout the rod, which is

reasonable for a given aggregation form. While this assumption neglects static disorder along the rod, it does not affect our results qualitatively. The different forward and backward rates are obtained from the geometry and the resulting dipole–dipole interaction. Because there are little details of energy transfer within the APC core, we focus on the PBS rod. Our results can be extended to heterogeneous rods adding phycoerythrin as building blocks.

The population dynamics along the rod is governed by the rate equation $\dot{P}(t) = -KP(t)$. The rate matrix,

$$K_{n \rightarrow m} = -k_{m \rightarrow n}^F + \delta_{nm}(k^D + \sum_{m'} k_{n \rightarrow m'}^F + \delta_{N, N_D} k^T) - \delta_{N, N_D} \delta_{n, \text{APC}} k^T \quad (1)$$

with n labeling the chromophores on the N th PC trimer, includes transfer rates to neighboring units (k^F obtained from Förster theory), decay rates (k^D) accounting for quenching and radiative decays, and trapping rates (k^T) from the PC trimer terminating the rod, N_D , to the APC core (see Figure 2 for a cartoon of the kinetic scheme). With the energy flow between PC rod and APC core being still unresolved, partly because of complex structure that could involve linker proteins,^{36–38} we use a phenomenological trapping rate from the last PC disk to APC, taking $k^T = 0.025 \text{ ps}^{-1}$, which corresponds to the lowest range of the experimentally measured range (0.025–0.056 ps^{-1}); cf. ref 39.

Considering the large distances separating the chromophores, the PC–PC transfer rate is evaluated from Förster theory (see ref 40 and, e.g., ref 41 for a review), which gives the rate between a donor D and an acceptor A as

$$k_{D \rightarrow A}^F = \frac{1}{\hbar^2 c} |V_{\text{dd}}|^2 \frac{\int_0^\infty d\omega E^D(\omega) I^A(\omega)}{\int_0^\infty E^D(\omega) d\omega \int_0^\infty I^A(\omega) d\omega} \quad (2)$$

The dipole–dipole coupling, $V_{\text{dd}} = \frac{\mu_D \mu_A}{4\pi\epsilon_0 n^2 R_{\text{DA}}^3}$, in units of cm^{-1} , and the orientation factor, $\kappa_{\text{DA}} = \hat{\mu}_D \cdot \hat{\mu}_A - 3(\hat{\mu}_D \cdot \hat{R}_{\text{DA}})(\hat{\mu}_A \cdot \hat{R}_{\text{DA}})$, are obtained from the structural data of the cyanobacterium *Thermosynechococcus vulcanus*⁴² (see also Figure S1 in the Supporting Information). The orientations of the transition dipole moments were estimated by fitting a line through the conjugated portions of the bilin chromophores. In addition to

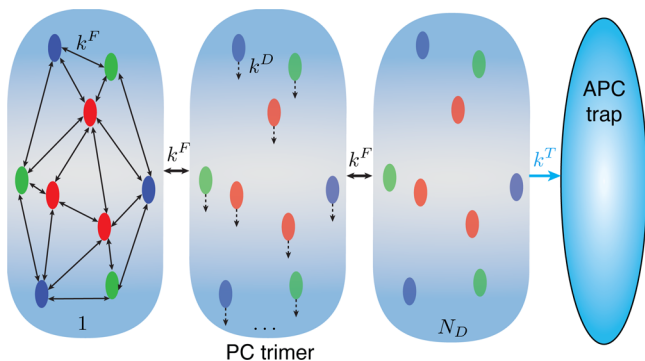


Figure 2. Cartoon of the kinetics scheme modeled here representing the rates for the chromophores (α_{84} , green; β_{84} , red; β_{155} , blue) forming each PC trimer. All chromophores transfer via Förster rates (k^F), and have a decay rate k^D accounting for quenching and spontaneous decay. Only the chromophores forming the last trimer, N_D , transfer to the APC trap, through k^T .

the symmetry used to build the hexamer, the rod is constructed repeating the hexamer disks with a pitch of 60.5 Å along the rod direction.⁴³ We use the screening factor and calculated dipole strength from ref 44, i.e., $n^2 = 2$ and $\mu = 13 \text{ D}$ for all chromophores—note that lower values have sometimes been used in the literature.⁴⁵ Quenching and radiative decay are taken from the experimental fitting of ref 46 as a biexponential decay, with time constants of 0.8 and 1.7 ns and a relative weight of 60 and 40%, respectively.

As mentioned above, the spectral properties of the bilin pigments highly depend on their environment, i.e., on the cyanobacteria strain and the aggregation form. Thanks to a recent theoretical analysis of experimental spectra in trimeric and hexameric forms,⁴⁶ the chromophore spectra in aggregate conformation are now available for *Th. vulc.* cyanobacterium. In the following, we will use these spectra—LS solvent, wet phase. We note that they are significantly different from those measured for isolated chromophores.³³ This difference is likely due to denaturation of the protein environment following the isolation process.

The detailed rates between each chromophore of the PC rod are given in the Supporting Information. The results are in quite good agreement with rates calculated for different species up to the hexameric structure, e.g., ref 32, especially considering that the rates are extremely sensitive to the structure. This is best illustrated in ref 32, where the rates for *A. quadruplicatum* are given for monomer, trimer, and hexamer aggregation states, for both the “old”⁴³ and the refined structure.⁴⁷ We see a variation of more than 2 orders of magnitude in the monomer rate, and a 25-fold factor in some of the trimer and hexamer rates for the different structures, although they correspond to the same species. The rates are therefore highly dependent on the structure resolution, and all the more so on the species.

To get the transfer efficiency, we first consider the case where the excitation is harvested by the i th trimer disk, and solve the dynamics for any rod length. Considering incoherent transport, the trap population collected in APC at steady state is obtained from $\int_0^\infty \dot{P}_{\text{APC}}(t) dt = \delta_{N, N_D} \sum_{n=1}^9 k_n^T P_n(t)$. It can be integrated directly using the rate equation to evaluate the population. This yields the disk efficiency, defined as the efficiency of transfer after excitation of the i th disk, as

$$\eta^{(i)} = \delta_{N, N_D} \sum_n k_n^T (K^{-1} \cdot P^{(i)}(0))_n \quad (3)$$

where $P^{(i)}(0)$ corresponds to an initial normalized excitation of disk i . The efficiency of the rod is then given by the average efficiency weighted by the harvesting cross section,⁴⁸ which is $N_D/(N_D + 1)$ in a rod of N_D PC trimers and one APC core. This gives the rod efficiency as $\eta = \frac{1}{N_D + 1} \sum_{i=1}^{N_D} \eta^{(i)}$.

The efficiency of transferring one excitation as a function of the rod length, defined in eq 3, is shown in Figure 3. It decreases as the rod length increases, even if the excitation is captured in the trimer neighboring the APC trap (see, e.g., $\eta^{(1)}$ in Figure 3a). This is due to leakage of the excitation to the neighboring trimer, opposite to the trap. As the excitation is captured further away from the trap, the transfer efficiency decreases due to losses in the form of quenching to the protein and radiative decays. The rod averaged efficiency, η , however, also accounts for the absorbing power that increases with the rod length. Because of a trade-off between the increasing absorbing power and the decreasing transport efficiency, there exists an optimal rod length for which the efficiency is maximal.

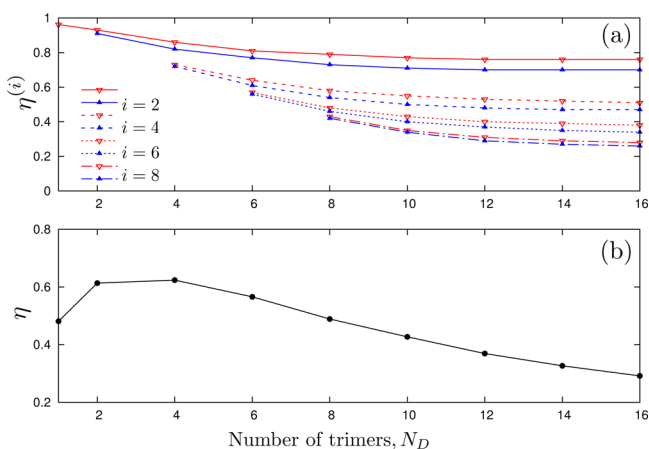


Figure 3. Efficiency (a) of the PC-trimer disk, $\eta^{(i)}$ (eq 3), for different locations of the initial excitation and (b) of the rod, η , defined as the efficiency of harvesting and transferring one excitation to the core, as a function of the number of PC trimers. Despite a disk efficiency decreasing with the rod length, the rod efficiency displays a maximum for a length of ~ 2 –4 trimers due to an increased harvesting cross section.

For the set of chosen parameters, we find this optimum is reached with $N_D = 4$ trimers—see Figure 3b. Results of the harvesting time, presented in the Supporting Information, further support this feature. Note that the results do not change significantly using a trapping rate of 0.056 ps^{-1} .

The total excitation transferred to the APC trap is readily given by $\chi_{\text{APC}} = \sum_i \eta^{(i)}$. Figure 4 shows that the excitation of the APC trap increases as the rod length increases due to higher absorption cross section. A lower intensity flux results in a lower transfer of excitation. It is possible to compensate for lower light intensity by increasing the rod length. As illustrated in Figure 4, maintaining the excitation of APC constant for 80% intensity can be done increasing the rod length from 2 to 3 hexamers.

Note that the results presented here are in line with those of ref 48, now extended to a biological system. There, the optimal length for a donor–acceptor system had been found in a 1D geometry. Here, we extended this to a quasi-2D geometry, and showed that there is an optimal number of donor disks for which the transfer to the acceptor is optimal. In addition, the APC population can be fitted into a biexponential (not presented here), such that two rates are mostly sufficient to account for the direct and indirect transfers, where the slower

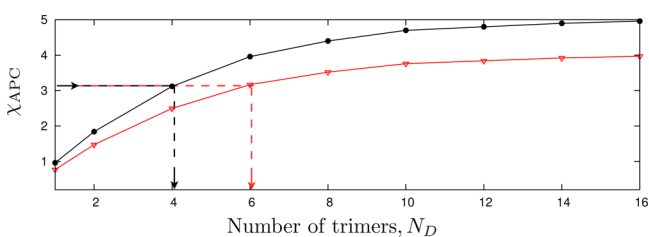


Figure 4. Total excitation transferred to the APC trap at steady state for 100% (black) and 80% (red) light intensity. The arrows indicate that, to keep a constant excitation reaching APC under varying excitation intensity, the rod length must be increased for decreasing light intensity (e.g., from 4 to 6 trimers in the particular example illustrated here).

rate integrates all back transfers, which is in agreement with refs 30 and 31.

STRUCTURAL CONSIDERATIONS FOR THE PBS ARRANGEMENT

The exact structure of PBS complexes is still an open question. Complete PBS structures were not resolved by X-ray crystallography, despite intensive efforts.⁴⁹ The best evidence currently available is from TEM image reconstruction studies. Current resolutions, of up to 3 PC hexamers⁵⁰ and 2 PC hexamers,⁵¹ still offer very limited structural models. We here use the transport properties to provide an additional argument.

Considering that the space between the thylakoid membranes is most likely packed with phycobiliproteins, we can infer the PC rod sizes from the length of this space. Table 1 presents such data extracted from electron microscopy and tomography of vitreous or cryo-fixed, freeze-substituted samples (see also Figure 6). This technique provides the most precise structural data because the cellular structures are preserved with high fidelity.^{52,53} The dimensions of PC hexamer and APC are very similar ($\sim 2 \times 3$ and 10 nm, respectively), and allow one to infer the plausible number of PC trimers forming the rod (N_D in Table 1). We thus propose two limiting cases of possible PBS geometries, depicted in the cartoon in Figure 1, to fill the space between the thylakoid membranes.

From a geometrical argument, stacking 3 APCs together, each modeled as a sphere of 10 nm diameter, we find that the APC core occupies about 16 nm of the vertical distance. This value supports the available structural models, in which APC is stacked to the height of two complexes of 16 nm (model A in Figure 1), to fit experiments. Indeed, this organization is supported by the measurement in the olive *Synechocystis* sp. PCC6803 mutant containing only APC, and where the distance between membranes was calculated to be ~ 32 nm (Table 1 and see also ref 54). The additional space in the wild-type species, which ranges from ~ 12 to ~ 26 nm, can be occupied by 4–9 PC trimers. We can imagine a different architecture where PC rods extend all the way to the opposite membrane face, generating space for up to 14 PC hexamers in a rod (model B, Figure 1, bottom). In reality, of course, any combination of the two extremes is possible, as is the currently used model. Judging by the experimental evidence, structures with shorter PC rods are more likely. Figure 5 shows the APC excitation for the two proposed models, which can be fitted as $P_{\text{APC}}(N_D) = a(1 - be^{-cN_D})$, using $\{a = 10.7, b = 1.0, c = 0.1\}$ for model A and $\{a = 5, b = 1.1, c = 0.3\}$ for model B. The comparison with the measured species is only indicative, as the rates have been

Table 1. Space between the Thylakoid Membranes Measured from the Cryo-Fixed Samples Presented in Figure 6^a

	cyanobacterial species	distance (nm)	N_D^A	N_D^B
(c)	<i>Synechocystis</i> sp. PCC6803 olive mutant (APC only)	31 ± 5		
(d)	<i>Synechococcus elongatus</i> PCC7942	45 ± 3	4	10
(b)	<i>Thermosynechococcus vulcanus</i>	53 ± 5	7	12
(e)	<i>Gloeobacter violaceus</i> PCC7421	55 ± 6	8	13
(a)	<i>Synechocystis</i> sp. PCC6803	58 ± 13	9	14

^aThe number of PC trimers for model A and B, N_D^A and N_D^B , respectively, has been inferred from the intra-membrane width without the APC complexes—see text for details.

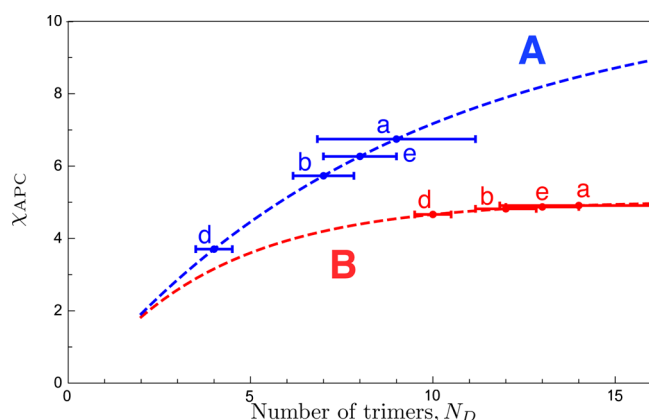


Figure 5. Total excitation at the APC trap(s) as a function of the PC rod length for model A (blue, 2 traps) and model B (red, 1 trap) along with the experimental data inferred from the intermembrane space, as presented in Table 1. The small letters label the different species shown in Figure 6.

evaluated from the structure of cyanobacterial *Thermosynechococcus vulcanus*. The stacking of model B results in an almost flat distribution and constant APC excitation across the presented species. Model A yields to a larger excitation reaching the APCs but requires the production of twice as many cores compared to model B. These results support shorter PC rods for larger excitation of the core, and are a further argument supporting the currently used model for PBS (model C in Figure 5) which consists of staggered PBS with 2–3 PCs, and is based on considerable experimental data.^{55,56}

In conclusion, we have developed a model to study the transport efficiency in the PBS complexes as a function of the rod length. Our kinetics analysis shows an optimal length for which the rod transport efficiency is maximal. It presents a

rationale to justify the evolutionary selected adaptation mechanism which consists of changing the PC:APC ratio as a response to the light intensity. This model can be extended to study organisms with much larger PBS structures composed of heterogeneous rods that contain additional PE phycobiliproteins,^{49,57} and study the PC:PE ratio as an adaptation to the light color. On the basis of the measurement of distances between the thylakoid membranes of various cyanobacterial species, we propose two limiting stacking models of the PBS complexes within the stromal. The kinetics analysis supports models with shorter rods, in line with the currently adopted PBS arrangement. Further considerations, such as the biological cost implying such a model and the free energy of the arrangements, are needed to discuss the most likely arrangement. There might be a trade-off between maximizing the excitation harvested and the actual cost of building super-complexes such as the APC core, which could help further resolve the exact structure of phycobilisome complexes.

■ ASSOCIATED CONTENT

📄 Supporting Information

The Supporting Information is available free of charge on the ACS Publications website at DOI: 10.1021/acs.jpcc.7b07781.

Additional information related to excitation transfer in isolated subunits, excitation transfer in the PC rod, and harvesting time (PDF)

■ AUTHOR INFORMATION

Corresponding Authors

*E-mail: achenu@mit.edu.

*E-mail: jjianshu@mit.edu.

ORCID

Aurélia Chenu: 0000-0002-4461-8289

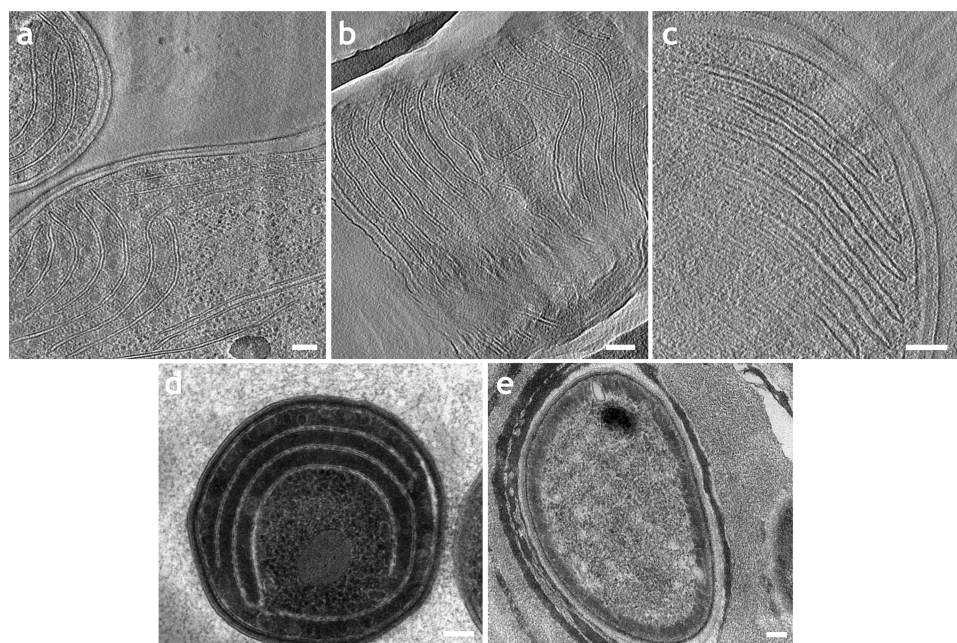


Figure 6. Thylakoid membrane organization of the organisms described in Table 1. (a) *Synechocystis* sp. PCC6803; (b) *Thermosynechococcus vulcanus*; (c) *Synechocystis* sp. PCC6803 “olive” (Δ PC) mutant, which is deficient in plastocyanin and, hence, lacks the peripheral rods of the phycobilisome;^{55,58} (d) *Synechococcus elongatus* PCC7942; (e) *Gloeobacter violaceus* PCC7421. (a–d) Tomographic slices (\sim 12 nm thick) of vitrified (a–c) or cryo-immobilized, freeze-substituted (d) samples. (e) TEM image of cryo-immobilized, freeze-substituted cells. Bars: 100 nm.

Notes

The authors declare no competing financial interest.

ACKNOWLEDGMENTS

We thank I. Eisenberg and F. Caycedo-Soler for sharing the data in ref 46 and for useful discussions. We acknowledge funding from NSF (Grant No. CHE- 1112825) and SMART IRG ID.

REFERENCES

- (1) Herrero, A.; Flores, E., Eds. *The cyanobacteria: molecular biology, genomics, and evolution*; Caister Academic Press: Norfolk, U.K., 2008.
- (2) Raps, S.; Kycia, J. H.; Ledbetter, M. C.; Siegelman, H. W. Light intensity adaptation and phycobilisome composition of *Microcystis aeruginosa*. *Plant Physiol.* **1985**, *79*, 983.
- (3) Grossman, A.; Schaefer, M.; Chiang, G.; Collier, J. The phycobilisome, a light-harvesting complex responsive to environmental conditions. *Microbiol. Rev.* **1993**, *57*, 725.
- (4) Bar-Eyal, L.; Eisenberg, I.; Faust, A.; Raanan, H.; Nevo, R.; Rappaport, F.; Krieger-Liszskay, A.; Sétif, P.; Thurotte, A.; Reich, Z.; Kaplan, A.; Ohad, I.; Paltiel, Y.; Keren, N. An easily reversible structural change underlies mechanisms enabling desert crust cyanobacteria to survive desiccation. *Biochim. Biophys. Acta, Bioenerg.* **2015**, *1847*, 1267.
- (5) Falkowski, P. G.; Dubinsky, Z. Light-shade adaptation of *Stylophora pistillata*, a hermatypic coral from the Gulf of Eilat. *Nature* **1981**, *289*, 172.
- (6) Cogdell, R. J.; Gardiner, A. T.; Hashimoto, H.; Brotsudarmo, T. H. P. A comparative look at the first few milliseconds of the light reactions of photosynthesis. *Photochem. Photobiol. Sci.* **2008**, *7*, 1150.
- (7) Plenio, M.; Huelga, S. Dephasing-assisted transport: Quantum networks and biomolecules. *New J. Phys.* **2008**, *10*, 113019.
- (8) Scholes, G. D.; Mirkovic, T.; Turner, D. B.; Fassioli, F.; Buchleitner, A. Solar light harvesting by energy transfer: from ecology to coherence. *Energy Environ. Sci.* **2012**, *5*, 9374.
- (9) Moix, J.; Wu, J.; Huo, P.; Coker, D.; Cao, J. Efficient energy transfer in light-harvesting systems, III: The influence of the eighth bacteriochlorophyll on the dynamics and efficiency in FMO. *J. Phys. Chem. Lett.* **2011**, *2*, 3045–3052.
- (10) Wu, J.; Liu, F.; Ma, J.; Silbey, R. J.; Cao, J. Efficient Energy Transfer in Light-Harvesting Systems: Quantum-Classical Comparison, Flux Network, and Robustness Analysis. *J. Chem. Phys.* **2012**, *137*, 174111.
- (11) Duffy, C. D. P.; Valkunas, L.; Ruban, A. V. Light-harvesting processes in the dynamic photosynthetic antenna. *Phys. Chem. Chem. Phys.* **2013**, *15*, 18752.
- (12) Blankenship, R. E. *Molecular Mechanism of Photosynthesis*; Blackwell Science: Oxford, U.K., 2002.
- (13) Walschaers, M.; Diaz, J.-D.-C.; Mulet, R.; Buchleitner, A. Optimally designed quantum transport across disordered networks. *Phys. Rev. Lett.* **2013**, *111*, 180601.
- (14) Kim, J.; McQuade, D. T.; Rose, A.; Zhu, Z.; Swager, T. M. Directing Energy Transfer within Conjugated Polymer Thin Films. *J. Am. Chem. Soc.* **2001**, *123*, 11488.
- (15) Polívka, T.; Sundström, V. Ultrafast Dynamics of Carotenoid Excited States-From Solution to Natural and Artificial Systems. *Chem. Rev.* **2004**, *104*, 2021–2071.
- (16) Balaban, T. S. Tailoring Porphyrins and Chlorins for Self-Assembly in Biomimetic Artificial Antenna Systems. *Acc. Chem. Res.* **2005**, *38*, 612.
- (17) Brédas, J.-L.; Norton, J. E.; Cornil, J.; Coropceanu, V. Molecular Understanding of Organic Solar Cells: The Challenges. *Acc. Chem. Res.* **2009**, *42*, 1691.
- (18) McConnell, I.; Li, G.; Brudvig, G. W. Energy Conversion in Natural and Artificial Photosynthesis. *Chem. Biol.* **2010**, *17*, 434.
- (19) Blankenship, R. E.; et al. Comparing Photosynthetic and Photovoltaic Efficiencies and Recognizing the Potential for Improvement. *Science* **2011**, *332*, 805.
- (20) Salleo, A. Organic electronics: something out of nothing. *Nat. Mater.* **2015**, *14*, 1077.
- (21) Rivnay, J.; Owens, R. M.; Malliaras, G. G. The Rise of Organic Bioelectronics. *Chem. Mater.* **2014**, *26*, 679.
- (22) Adir, N. *Structure of the Phycobilisome Antennae in Cyanobacteria and Red Algae*; 2008; pp 243–274.
- (23) De Lorimier, R.; Smith, R.; Stevens, S., Jr. Regulation of phycobilisome structure and gene expression by light intensity. *Plant Physiol.* **1992**, *98*, 1003–1010.
- (24) Stowe, W.; Brodie-Kommit, J.; Stowe-Evans, E. Characterization of complementary chromatic adaptation in *Gloeotrichia* UTEX 583 and identification of a transposon-like insertion in the *cpeBA* operon. *Plant Cell Physiol.* **2011**, *52*, 553–562.
- (25) Wiltbank, L.; Kehoe, D. Two cyanobacterial photoreceptors regulate photosynthetic light harvesting by sensing teal, green, yellow, and red light. *mBio* **2016**, *7*, e02130-15.
- (26) Kehoe, D.; Gutu, A. Responding to color: The regulation of complementary chromatic adaptation. *Annu. Rev. Plant Biol.* **2006**, *57*, 127.
- (27) Chakdar, H. In *Cyanobacterial Phycobilins: Production, Purification, and Regulation*; Shukla, P., Ed.; Springer: India, 2016.
- (28) Adir, N.; Dines, M.; Klartag, M.; McGregor, A.; Melamed-Frank, M. In *Complex Intracellular Structures in Prokaryotes*; Shively, J. M., Ed.; Springer: Berlin, Heidelberg, 2006; pp 47–77.
- (29) Adir, N.; Dobrovetsky, Y.; Lerner, N. Structure of c-phycocyanin from the thermophilic cyanobacterium *Synechococcus vulcanus* at 2.5 Å: structural implications for thermal stability in phycobilisome assembly. *J. Mol. Biol.* **2001**, *313*, 71.
- (30) Holzwarth, A. R.; Wendler, J.; Suter, G. W. Studies on chromophore coupling in isolated phycobiliproteins: II. Picosecond energy transfer kinetics and time-resolved fluorescence spectra of C-phycocyanin from *Synechococcus* 6301 as a function of the aggregation state. *Biophys. J.* **1987**, *51*, 1.
- (31) Suter, G. W.; Holzwarth, A. R. A Kinetic Model for the Energy Transfer in Phycobilisomes. *Biophys. J.* **1987**, *52*, 673.
- (32) Sauer, K.; Scheer, H. Excitation transfer in C-phycocyanin. Förster transfer rate and exciton calculations based on new crystal structure data for C-phycocyanins from *Agmenellum quadruplicatum* and *Mastigocladus laminosus*. *Biochim. Biophys. Acta, Bioenerg.* **1988**, *936*, 157.
- (33) Debreczeny, M. P.; Sauer, K.; Zhou, J.; Bryant, D. A. Monomeric C-phycocyanin at room temperature and 77 K: resolution of the absorption and fluorescence spectra of the individual chromophores and the energy-transfer rate constants. *J. Phys. Chem.* **1993**, *97*, 9852.
- (34) Glazer, A.; Chan, C.; Williams, R.; Yeh, S. W.; Clark, J. Kinetics of energy flow in the phycobilisome core. *Science* **1985**, *230*, 1051.
- (35) Grabowski, J.; Gantt, E. Photophysical properties of phycobiliproteins from phycobilisomes: fluorescence lifetimes, quantum yields, and polarization spectra. *Photochem. Photobiol.* **1978**, *28*, 39.
- (36) Liu, L.-N.; Chen, X.-L.; Zhang, Y.-Z.; Zhou, B.-C. Characterization, structure and function of linker polypeptides in phycobilisomes of cyanobacteria and red algae: An overview. *Biochim. Biophys. Acta, Bioenerg.* **2005**, *1708*, 133.
- (37) Tal, O.; Trabelcy, B.; Gerchman, Y.; Adir, N. Investigation of phycobilisome subunit interaction interfaces by coupled cross-linking and mass spectrometry. *J. Biol. Chem.* **2014**, *289*, 33084.
- (38) David, L.; Prado, M.; Arteni, A.; Elmlund, D.; Blankenship, R.; Adir, N. Structural studies show energy transfer within stabilized phycobilisomes independent of the mode of rod-core assembly. *Biochim. Biophys. Acta, Bioenerg.* **2014**, *1837*, 385.
- (39) Li, Y.; Wang, B.; Ai, X.-C.; Zhang, X.-K.; Zhao, J.-Q.; Jiang, L.-J. Spectroscopic investigation on the energy transfer process in photosynthetic apparatus of cyanobacteria. *Spectrochim. Acta, Part A* **2004**, *60*, 1543.
- (40) Förster, T. In *Modern Quantum Chemistry: Istanbul Lectures - Part III, Action of Light and Organic Crystals*; Cinanogu, O., Ed.;

Academic: New York, 1965; Chapter Delocalized Excitation and Excitation Transfer, pp 93–137.

(41) Scholes, G. D. Long-Range Resonance Energy Transfer in Molecular Systems. *Annu. Rev. Phys. Chem.* **2003**, *54*, 57–87.

(42) Adir, N.; Dobrovetsky, E.; Lerner, N. Crystal Structure of C-Phycocyanin of *Synechococcus Vulcanus* at 2.5 Ångstroms. PDB file 1I7Y, 2001.

(43) Schirmer, T.; Huber, R.; Schneider, M.; Bode, W. Crystal Structure Analysis and refinement at 1.5 Å of hexameric C-phycocyanin from the Cyanobacterium *Agmenellum quadruplicatum*. *J. Mol. Biol.* **1986**, *188*, 651.

(44) Ren, Y.; Chi, B.; Melhem, O.; Wei, K.; Feng, L.; Li, Y.; Han, X.; Li, D.; Zhang, Y.; Wan, J.; Xu, X.; Yang, M. Understanding the electronic energy transfer pathways in the trimeric and hexameric aggregation state of cyanobacteria phycocyanin within the framework of Förster theory. *J. Comput. Chem.* **2013**, *34*, 1005.

(45) Womick, J.; Moran, A. Exciton coherence and energy transport in the light-harvesting dimers of allophycocyanin. *J. Phys. Chem. B* **2009**, *113*, 15747.

(46) Eisenberg, I.; Caycedo-Soler, F.; Harris, D.; Yochelis, S.; Huelga, S. F.; Plenio, M. B.; Adir, N.; Keren, N.; Palti, Y. Regulating the Energy Flow in a Cyanobacterial Light-Harvesting Antenna Complex. *J. Phys. Chem. B* **2017**, *121*, 1240.

(47) Schirmer, T.; Bode, W.; Huber, R. Refined three-dimensional structures of two cyanobacterial C-phycocyanins at 2.1 and 2.5 Å resolution: A common principle of phycobilin-protein interaction. *J. Mol. Biol.* **1987**, *196*, 677.

(48) Kim, J.-H.; Cao, J. Optimal Efficiency of Self-Assembling Light-Harvesting Arrays. *J. Phys. Chem. B* **2010**, *114*, 16189.

(49) Marx, A.; David, L.; Adir, N. In *The Structural Basis of Biological Energy Generation*; Hohmann-Marriott, M., Ed.; Springer: 2014; Chapter Piecing Together the Phycobilisome, pp 59–76.

(50) Arteni, A. A.; Ajlani, G.; Boekema, E. J. Structural organisation of phycobilisomes from *Synechocystis* sp. strain PCC6803 and their interaction with the membrane. *Biochim. Biophys. Acta, Bioenerg.* **2009**, *1787*, 272.

(51) Chang, L.; Liu, X.; Li, Y.; Liu, C.-C.; Yang, F.; Zhao, J.; Sui, S.-F. Structural organization of an intact phycobilisome and its association with photosystem II. *Cell Res.* **2015**, *25*, 726.

(52) Nevo, R.; Charuvi, D.; Shimoni, E.; Schwarz, R.; Kaplan, A.; Ohad, I.; Reich, Z. Thylakoid membrane perforations and connectivity enable intracellular traffic in cyanobacteria. *EMBO J.* **2007**, *26*, 1467.

(53) Nevo, R.; Charuvi, D.; Chuartzman, S. G.; Shimoni, E.; Tsabari, O.; Reich, Z. In *Lipids in photosynthesis: Essentials and regulatory functions*; Wada, H., Murata, N., Eds.; Springer: 2009; Chapter Architecture and plasticity of thylakoid membrane networks, p 295.

(54) Liberton, M.; Page, L. E.; O'Dell, W. B.; O'Neill, H.; Mamontov, E.; Urban, V. S.; Pakrasi, H. B. Organization and flexibility of cyanobacterial thylakoid membranes examined by neutron scattering. *J. Biol. Chem.* **2013**, *288*, 3632.

(55) Olive, J.; Ajlani, G.; Astier, C.; Recouvreur, M.; Vernotte, C. Ultrastructure and light adaptation of phycobilisome mutants of *Synechocystis* PCC 6803. *Biochim. Biophys. Acta, Bioenerg.* **1997**, *1319*, 275.

(56) Van De Meene, A. M.; Sharp, W. P.; McDaniel, J. H.; Friedrich, H.; Vermaas, W. F.; Roberson, R. W. Gross morphological changes in thylakoid membrane structure are associated with photosystem I deletion in *Synechocystis* sp. PCC 6803. *Biochim. Biophys. Acta, Biomembr.* **2012**, *1818*, 1427.

(57) Ong, L.; Glazer, A. Phycoerythrins of marine unicellular cyanobacteria. I. Bilin types and locations and energy transfer pathways in *Synechococcus* spp. phycoerythrins. *J. Biol. Chem.* **1991**, *266*, 9515.

(58) Elmorjani, K.; Thomas, J.-C.; Sebban, P. Phycobilisomes of wild type and pigment mutants of the cyanobacterium *Synechocystis* PCC 6803. *Arch. Microbiol.* **1986**, *146*, 186.